Enhanced PEC Characteristics of Elemental 2D Materials Thin Film Electrodes by Bottom-Up Approach Monolayer Deposition

M. Abdurrahman

Department of Physics, Faculty of Physical Science, Federal University, Dutse, Nigeria

*Corresponding author; Email: Msabdurrahaman@yahoo.com

Article Info

Article history:

Received , 18/10/2025
Revised , 15/11/2025
Accepted , 11/12/2025

Keywords:

Thin film;
Counter electrode;
Chemical etching;
Elemental 2D;
Chalcogenide;

ABSTRACT

The direct current conductivity and electrical power conversion efficiency of elemental 2D materials thin films were fabricated and investigated for the solar cell efficiency. We optimized the deposition of 2D elements such as HgO, $Fe_2(SO_4)_3$, $ZnCl$, Cu_2O and Cu_2S to create high-quality thin films using three different methods of chemical vapor deposition. The optical properties showed that as the amount of 2D materials increased, the band gap of the films became smaller. In our photoconduction tests, we found that when exposed to light, the current increased steadily with higher solar irradiance, while photocurrent changed with the level of solar irradiance applied. We characterized the PEC solar cell made from HgO, $Fe_2(SO_4)_3$, $ZnCl$, Cu_2O and Cu_2S thin films by measuring key factors such as open-circuit voltage (Voc), short-circuit current (Isc), maximum power (Pmax), fill factor (ff), and efficiency (η %). We used a sample cell area of 2 cm² and tested it under various levels of solar irradiance measured in W/m². The results showed a fill factor of 0.40 % and a conversion efficiency of 5.50 % for one specific composition based on I-V measurements.

I. Introduction

Many researchers are exploring the use of thin films made from metal chalcogenides (MX, where M represents metals like Pb, Cd, Cu, Zn, and X stand for elements like S, Se, or Te) as an alternative to traditional p–n junction photovoltaics (PV) in photoelectrochemical (PEC) conversion processes [1]. These thin films can achieve high efficiencies of up to 29% [2,3]. They have been studied for various applications because their band gap values align with visible light that comes freely from the sun. Additionally, they are simple to produce using common starting materials and do not require special conditions. However, their medium band gap values make them vulnerable to degradation when operating under PEC conditions [4,5]. Over the last few decades, II-VI and IV-VI group compound materials have gained attention for their clear physical properties, such as high efficiency, strong optical absorbance, and direct band gaps. These traits make them promising for a variety of optoelectronic uses, including photodetectors, photovoltaic devices, lasers, infrared detectors, solar control coatings, and solar cells [6-9]. These materials can be applied in thin film form using several techniques like vacuum deposition, chemical bath deposition, chemical vapor deposition, electro-deposition, spray pyrolysis, and sol-gel methods [10-18].

$Pb_xCd_{1-x}S$ thin films are recognized as important high-tech materials because they are used in many optical and

electronic devices [19]. Among the II-VI semiconductors, Cadmium sulfide (CdS) thin films stand out as a typical n-type material with applications in large-area electronic devices and solar cells. CdS has a wide direct band gap of 2.42 eV, making it suitable to be used as a window material alongside other semiconductor like Cu_2S [20]. A photoelectrochemical (PEC) cell is a type of solar device that combines semiconductor materials with an electrolyte interface to convert solar energy into electrical energy.

As an advanced microelectronic technology, PEC can be utilized for both generating voltage from light and converting chemical energy. [21] Currently, silicon is the most common material used for PEC fabrication; however, its cost is quite high for large-scale production. [22] Therefore, researchers are actively looking for new materials that can efficiently convert energy at a more affordable price without losing performance. [23] Due to the effort in discovering new materials, Transition Metal Chalcogenides (TMC) are seen as the best semiconductor materials for photoelectrochemical (PEC) applications. TMC is a combination of transition metals from group 10 and chalcogenides from group 16, represented as MX_2 (where M can be Cd, Mo, Zn, etc., and X can be S, Se, or Te). TMC shows remarkable optical, electrical, and semiconductor qualities, especially when in thin film form. [24] This progress has encouraged many researchers to study TMC thin films for PEC applications like CdS, [25] CdSe,[26] ZnS,[27] SnS [28] and others. Cadmium chalcogenides are the most commonly used TMC materials for energy conversion because they have high photo conversion efficiency [26,29]. Thin films of chalcogenides can be made using methods such as spray pyrolysis, electrochemical deposition [30], and sputtering [31]. The goal of this study was to enhance the photovoltaic performance of solar cells based on PEC solar cells made from copper oxide, particularly focusing on increasing photoconversion efficiency. Using a heteroepitaxial layer alters how Cu_2O window layers grow and leads to improvements in photovoltaic performance.

II. Research Method

For a better thoughtful of thermal oxidation mechanism, we introduce here a schematic of the surface oxidation process of thin copper films and the effect of oxidation temperature, as shown in Figure 1. Exposure of a fresh copper film to air ambient results in a spontaneous native oxide formation, which later acts as a diffusion barrier for O_2 and prevents the further oxidation. The thermal energy at 150 ˚C, overcomes the diffusion barrier and Cu_2O formation starts. However, activation energy of CuO formation demands a higher thermal energy (325 ˚C). In all cases, a longer duration of oxidation results in a thicker oxide layer whereas the oxidation temperature determines the oxide phase.

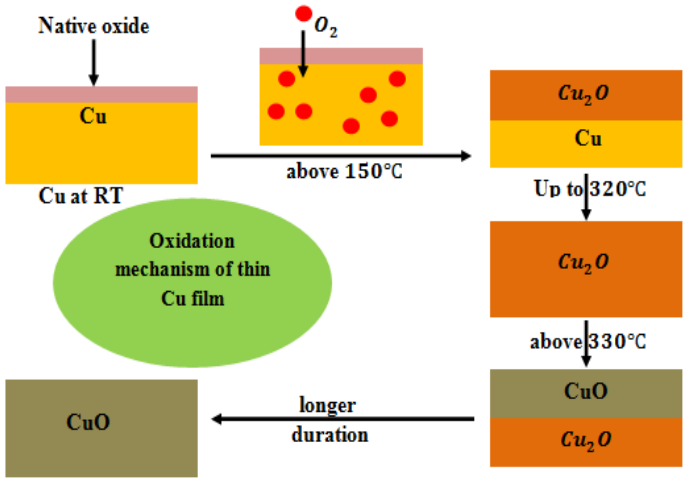

Figure 1. Oxide growth schematics of thin Cu film during thermal oxidation in air.

$Cu_2S/Cu_2O|1g$ NaCl|C(copper) solar cells were grown by chemical vapour deposition (CVD). Details of the surface enhancement and the approximate value of the achieved parameters of the synthesized layers are shown in Table 1. The schemes of the thin-film solar cells are shown in Figure 1

Table 1. The schemes of the thin-film solar cells.

S/N	Sample	$I_{sc}(mA)$	$V_{oc}(mV)$	$\eta(\%)$	FF
1	HgO	0.87	78	4.30	0.20
2	$Fe_2(SO_4)_3$	0.75	65	5.40	0.46
3	$ZnCl$	5.36	298	0.79	0.20
4	Cu_2O	0.50	35	1.7	0.41
5	Cu_2S	1.00	61	5.50	0.40

Starting materials HgO, $Fe_2(SO_4)_3$, $ZnCl$, Cu_2O and Cu_2S, redox couple materials, and organic solvents were used in their pure forms. The substrates were pre-cleaned by washing them several times with distilled water and methanol then soaked them in dilute HCl for 4 seconds. After that, we dried them using tissue paper before proceeding with film deposition.

II.1. Electrode Preparation HgO, $Fe_2(SO_4)_3$, $ZnCl$, Cu_2O and Cu_2S

HgO, $Fe_2(SO_4)_3$, $ZnCl$, Cu_2O and Cu_2S thin films were thermally evaporated onto Cu_2O using a method modified from literature [32]. First, we cut copper foil into squares measuring 2 cm x 2 cm. Next, we cleaned these pieces using ultrasonic waves in a solution of 2-propanol, ethanol, and distilled water. Following this, we preheated the substrates in a microwave oven at 250°C for 10 minutes to remove any remaining water and unwanted solvents from their surfaces. We then placed them in a clean envelope as we waited for the oxidation temperature to be reached. The samples were positioned between ceramic crucibles and put into a high-temperature furnace set to 950°C (figure 2), where they oxidized for 8 minutes. Right after that, we quenched them in cold distilled water and dried them by placing them between tissue papers before letting them air dry. The films deposited at 950°C were annealed at 450°C under oxygen flow for 60 minutes. Finally, we cooled the annealed films back down to room temperature.

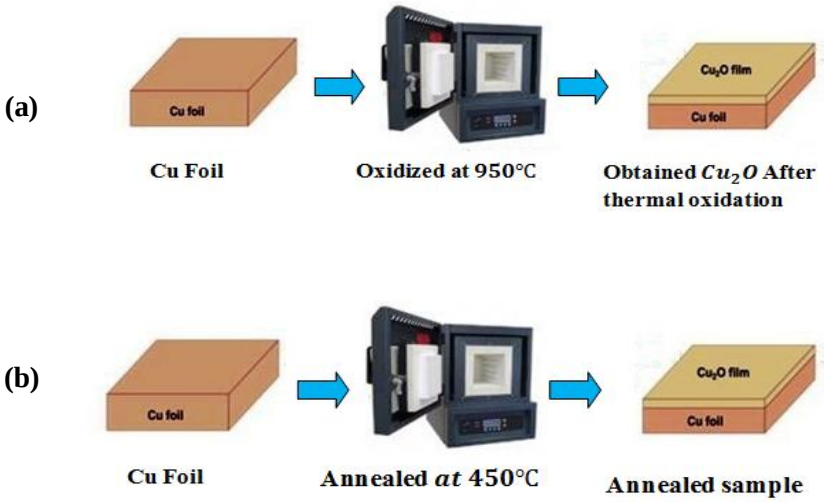

Figure 2: (a) Thermal oxidation of the samples at 950°C (b) Annealing of the samples at 450°C

II.2. Results and discussion

HgO, $Fe_2(SO_4)_3$, $ZnCl$, Cu_2O and Cu_2S thin films were characterized using various techniques. We focused on how different preparation conditions, like deposition time and pre-annealing temperature, affect the characteristics of the film electrodes. We examined the impact of coating on all five samples that were synthesized. Next, we conducted a Photoelectrochemical (PEC) study on different electrodes to observe how treatment influenced their characteristics. Thus, we carried out characterization and PEC studies only on the five samples mentioned earlier.

1) Fabrication and characterization of PEC cell

We used a two-electrode cell with five different reference electrodes, each used separately, along with a copper sheet as the counter electrode. Figure 3 shows the two electrode setups used in this experiment. The materials HgO, $Fe_2(SO_4)_3$, $ZnCl$, Cu_2O and Cu_2S and served as photoanodes, while copper acted as the counter electrode, and sodium chloride was utilized as the liquid electrolyte. The space between the two electrodes during illumination was set at 5.0 cm. [32] We determined the type of conductivity displayed by the photoelectrode by checking the polarity of the electromotive force (emf) developed in the PEC cell when illuminated. We plotted the current–voltage (I–V) characteristics under light exposure. Additionally, we obtained power output characteristics for the PEC cell under various lighting conditions. We calculated both the fill factor and power conversion efficiency from these photovoltaic power output characteristics. The maximum power was assessed based on photoresponse measurements. Finally, we measured spectral response by determining short circuit current and open circuit voltage as functions of incoming light.

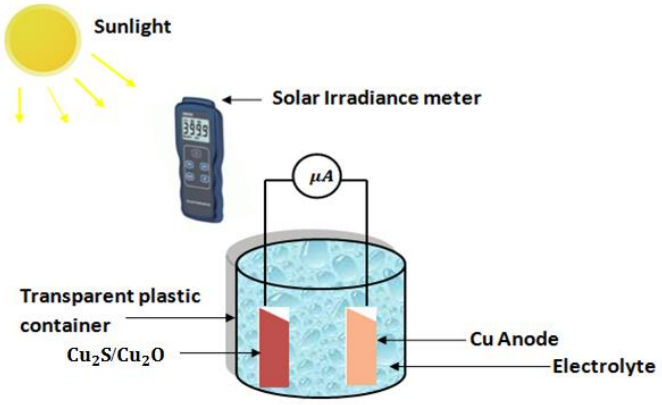

Figure 3. PEC analysis of the synthesized samples

Figure 4. Show the current-voltage (I-V) curves for the deposited Cu_2S/Cu_2O thin film under a light with visible light. All the films under visible illumination in terms of open-circuit voltage (Voc), short circuit current density (Isc), fill factor (ff) and electron conversion efficiency (η) are matched in table 1. These (I-V) curves in the dark indicate good junction rectification property. From the I-V measurements it is observed that the higher magnitudes fill factor 0.40 % and conversion efficiency 5.50 % is obtained for composition Cu_2S/Cu_2O. This is a significant improvement as compared to other compositions [32].

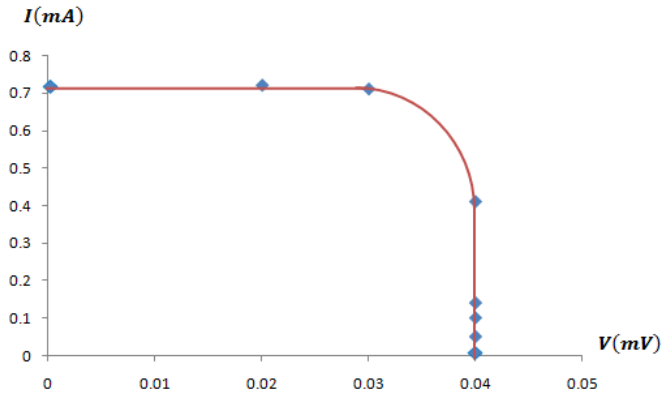

Figure 4. The graph of Cu-**Cu_2S/Cu_2O** photoelectrochemical solar cell after surface modification.

The improvement in the efficiency of the solar cell is a result of good crystalline structures of the thin film during deposition. This may result in an increase in the resistance due to the good quality of the films. This also implies that no holes or cracks were found in the films, which may cause transmission loss. The solar cell efficiency in the present study is higher and more promising than some other solar cell fabricated by the chemical vapour deposition technique.

2) FTIR analysis

Figure five (5) shows the FTIR spectrum of Cu_2S/Cu_2O created in an oven using direct transport on a substrate that was heated for one hour. There is a peak at 1106 cm^{-1} linked to the S-O vibrational mode and a Cu-S sulfide oxide band at 745 cm^{-1}. A clear peak at 630 cm^{-1} represents the Cu-O vibrational mode in the Cu_2O phase, as identified by Ji [33]. Additional features at 1624.74 and 3445.37 cm^{-1} relate to -OH bending and stretching vibrations caused by water, as noted by Ansari et al. [34]. The band at 3417 cm^{-1} matches the stretching vibration of –OH groups, while there is no band for –NH stretching vibrations; however, N–H bending vibrations appear at 1544 cm^{-1}. The shoulder observed at 1439 cm^{-1} is due to C–H bending vibrations. The shoulder at 1439 cm^{-1} comes from C–H bending vibrations. The band for O–H in-plane bending vibrations is missing, but we can see bands for C–O and C–C stretching vibrations in the 1150–950 cm^{-1} range. [35,36,37] noted that the band for C–O out-of-plane bending vibrations is not detected. A combination band for $–CH_2$, –OCH, and –CCH bending vibrations appears at 1461 cm^{-1}, while the deformation bands for –OCH, –COH, and –CCH are found at 1383 cm^{-1} according to Ibrahim et al. [38]. The absorption band between 1622-1383 cm^{-1} relates to the deformation vibrations of water residue d(HOH). A broad absorption band around 3417 cm^{-1} shows up in the near-infrared spectra, indicating stretching vibrations of bound OH groups as shown by Keiser et al. [39].
The peaks at 3488 cm^{-1} and 1637 cm^{-1} are not related to hydrogen bond vibrations or surface water in materials as indicated by Li et al. [40]. In the range of 2500-4000 cm^{-1}, we can observe peaks from single bonds. Hydrogen bonds create a broad absorption band between 3650 and 3250 cm^{-1} as shown by Nandiyanto et al. [41]. For hydroxyl compounds, it has been confirmed that this occurs due to spectral presence at frequencies of 1600–1300, 1200–1000, and 800–600 cm^{-1}.

Oxygen-related bonding was detected due to a sharp peak around 3506 cm^{-1}. Aromatic structures showed a peak at 3088 cm^{-1}, which falls between 3000 and 3200 cm^{-1}, as noted by Nandiyanto et al. [42]. There were also weak peaks below 3000 cm^{-1} related to C-C bonds. No distinct peak for aldehyde appeared between 2700 and 2800 cm^{-1}. A range of triple bonds (2000-2500 cm^{-1}) indicated the presence of C≡C bonds in the sample, as reported by [41,42]. In the double bond region (1500-2000 cm^{-1}), a strong, sharp peak suggested a double bond's presence, indicating that there could be carbonyl double bonds from aldehydes, esters, ketones, or carboxylic acids. The material being analyzed contains water components. Compounds associated with vinyl were found around 800 cm^{-1}. A strong signal confirmed the presence of aromatic rings, as shown by [43]. Additionally, there was a CH_2/CH_3 peak at 2900 cm^{-1}.

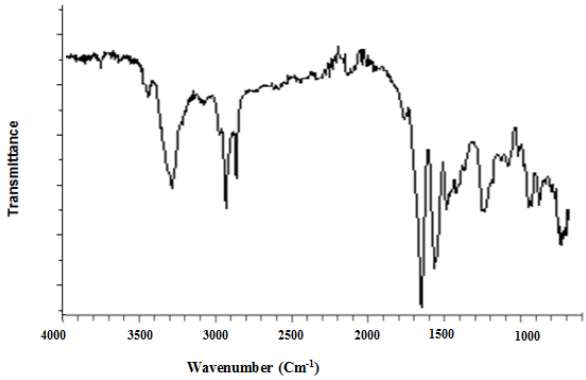

Figure 5. The graphical record of Fourier transforms invisible or infrared (FTIR) spectroscopy of analyzed Cu_2S/Cu_2O

III. Conclusion

HgO, $Fe_2(SO_4)_3$, $ZnCl$, Cu_2O and Cu_2S binary thin films of various materials are created using the chemical vapor deposition technique, and these films exhibit semiconducting properties. The composition of all elemental 2D materials varies significantly in the binary deposition of the HgO/Cu_2O, $Fe_2(SO_4)_3/Cu_2O$, $ZnCl/Cu_2O$, Cu_2O/Cu_2O and Cu_2S/Cu_2O thin films. As the films grow, their colors change from reddish-brown to yellowish and black. The optical band gap of the deposited films is found to decrease. Additionally, the electrical conductivity in all synthesized thin film samples decreases consistently as the composition increases. It is also

noted that activation energy drops with higher composition in all thin films. In a study on photoconductivity, photocurrent increases when voltage is applied under light, and current rises almost linearly with voltage but decreases as the composition of the thin film increases. This pattern indicates that the films have non-ohmic behavior. In this study, a photoelectrochemical (PEC) solar cell with five different structures was made using the CBD technique. Because of the high quality of the thin films produced, the PEC solar cell demonstrates a conversion efficiency of 5.50%.

Acknowledgements

I would like to show gratitude Federal University Dutse and Tertiary Educational Fund, for providing favorable environment, equipment during the researchwork.

References

[1] Z. Tachan, M. Shalom, I. Hod, S. Rühle, S. Tirosh, A. Zaban, PbS as a highly catalytic counterelectrode for polysulfide-based quantum dot solar cells, J. Phys. Chem. C 115 (2011) 6162–6166.
[2] A. Richter, M. Hermle, S.W. Glunz, Reassessment of the limiting efficiency for crystalline silicon solar cells, IEEE J. Photovolt. 3 (2013) 1184–1191.
[3] Y. Guo, A.L. Porter, L. Huang, Nanotechnology enhanced thin-film solar cells: analysis of global research activities with future prospects, in: Proceedings of the 18th International Conference for the International Association of Management of Technology, Orlando, FL, 2009.
[4] J. Portier, H. Hilal, I. Saadeddin, S. Hwang, M. Subramanian, G. Campet, Thermodynamic correlations and band gap calculations in metal oxides, Prog. Solid State Chem. 32 (2004) 207–217.
[5] H. Sabri, S. Saleh, A. Zyoud, N.N. Abdel-Rahman, I. Saadeddin, G. Campet, D. Park, M. Faroun, H.S. Hilal, Enhancement of CdSe film electrode PEC characteristics by metalloporphyrin/polysiloxane matrices, Electrochim. Acta 136 (2014) 138–145.
[6] J. F. Mohammad, H. S. Al-jumaili, S. M. Abed, Int. J. of App. or Inno. In Engg and Mgmt., (2014) 3.
[7] R. Y. Mohammed, S. Abduol, A. M. Mousa, Int. Lett. of Chem., Phy. And Astr. 10 (2014) 91.
[8] A. S. Obaid, M. A. Mahdi, Z. Hassan, M. Bououdina,Int. Conf. on Edu., App. Sci. and Mgmt., Dubai (UAE), (2012).
[9] V. Popescu, G. L. Popescu, J. of optoele. And Adv. Mater. 13 (2011) 926.
[10] V. Popescu, H. I. Nascu, E. Darvasi, J.of Optoele. And Adv. Mater., 8 (2006)1187.
[11] M. Kamruzzaman, R. Dutta, J. Podder, Semi's., 46 (7) (2012) 979-983.
[12] M. A. Barote, A. A. Yadav, E. U. Masumdar, Chalco. Lett., 8 (2) (2011) 129-138.
[13] M. A. Mohammed, A. M. Mousa, J. P. Ponpon, J. of Semi.Tech.and Sci., 9 (2009) 117.
[14] H. S. AL-Jumaili, App. Phy. Res., 4 (2012) 75-82.
[15] K. E. Suryavanshi, R. B. Dhake, A. M. Patil, Int. J. of Adv. Sci. and Tech. Res., 4 (2) (2014) 858.
[16] E. Omotoso, G. A. Adegboyega, M. A. Eleruja, B. Olofinjana, O. O. Akinwunmia, O. O. Ilori, B. A. Taleatu, E. O. B. Ajayi, J. of Non-Oxide Glasses, 5 (1) (2013) 9.
[17] M. M. Abdulla, N. H. Hasan, H. I. Mohammed, G. H. Mohamed, K. A. Al-Hamdani, A. F. Abdulameer, J. of Elect. Devi, 12 (2012) 761.
[18] S. Lindroos, J. Puiso, S. Tamulevicius, M. Leskela, Solid State Pheno., 99 (2004) 243.
[19] J. C.Osuwa, C. I. Oriaku, E. C. Mgbaja, Chalco. Lett.,7 (2010) 679.
[20] Y. A. Salazar, R. Patino, J. L. Pena, W. Cauich, A. I. Oliva, Brazilian Journal of Physics, 36 (2006) 1058 - 1061.

[21] Yadav AA, Masumdar EU. Photoelectrochemical performances of n-$CdS_{1-x}Se_x$ thin flms prepared by spray pyrolysis technique. Sol Energy. 2010 ;84(8) :1445–1452

[22] Anuar K, Tan WT, Atan MS, et al. Cyclic Voltammetry Study of Copper Tin Sulfde Compounds. Pac J Sci Technol. 2007; 8:252–260.

[23] Duchatelet A, Sidali T, Loones N, et al. 12.4% Effcient Cu(In,Ga) Se_2 solar cell prepared from one step electrodeposited Cu–In–Ga oxide precursor layer. *Sol Energy Mater Sol Cells*. 2013;119:241–245.

[24] Anand TJS, Shariza S. A study on molybdenum sulphoselenide (MoS_xSe_{2-x}, $0 \leq x \leq 2$) thin films : Growth from solution and its properties. *Electrochim Acta*. 2012;81:64–73.

[25] Yadav AA, Masumdar EU. Photoelectrochemical investigations of cadmium sulphide (CdS) thin flm electrodes prepared by spray pyrolysis. *J Alloys Compd*. 2011;509(17):5394–5399.

[26] Hankare PP, Jadhav BV, Chate PA, et al. Synthesis and characterization of chemically deposited nickel substituted CdSe thin film. *J Alloys Compd*. 2011;509(6):2948–2951.

[27] Luque PA, Quevedo-Lopez MA, Olivas A. Influence of deposition time on ZnS thin film growth over SiO_2 and glass substrates. *Mater Lett*. 2013;106:49–51.

[28] Jain P, Arun P. Influence of grain size on the band-gap of annealed SnS thin films. *Thin Solid Films*. 2013;548:241–246.

[29] Hankare P, Bhuse V, Garadkar K, et al. Low temperature route to grow polycrystalline cadmium selenide and mercury selenide thin films. *Mater Chem Phys*. 2003;82(3):711–717.

[30] Kokate AV, Asabe MR, Delekar SD, et al. Photoelectrochemical properties of electrochemically deposited CdIn2S4 thin films. J Phys Chem Solids. 2006;67(11):2331–2336.

[31] Volobujeva O, Altosaar M, Raudoja J, et al. SEM analysis and selenization of Cu–In alloy flms produced by co-sputtering of metals. *Sol Energy Mater Sol Cells*. 2009;93(1):11-14.

[32] M. Abdurrahman**,** F.W Burari, & O.W Olasoji Influence of heteroepitaxial growth of 2D materials on catalytic performance of ZnO and its applications in photoelectrochemical solar cell Algerian Journal of Materials Chemistry 06 (2023) 49–58, EISSN 2716-9472 (Online) **|** ISSN 2661- 7196 (Print), https://doi.org/10.5281/zenodo.10074427

[33] Ji, C.; Yin, S.-N.; Sun, S.; Yang, S. (2018). An in situ mediator-free route to fabricate Cu_2O/g-C_3N_4 type-II heterojunctions for enhanced visible-light photocatalytic H_2 generation. Appl. Surf. Sci, 434, 1224-1231.

[34] Ansari, A.; Ali, A.; Asif, M.; Shamsuzzaman, S. (2018). Microwaveassisted MgO NP catalyzed one-pot multicomponent synthesis of polysubstituted steroidal pyridines. New J. Chem. 42, 184-197.

[35] Prakash. I, Muralidharan. P, Nallamuthu. N, Venkateswarlu. M, Satyanarayana. N, (2007). Preparation and characterization of nanocrystallite size cuprous oxide, Mater. Res. Bull. 42 1619–1624.

[36] Yang. H, Ouyang. J, Tang A, Xiao. Y, Li. X, Dong. X, Yu. Y, (2006). Electrochemical synthesis and photocatalytic property of cuprous oxide nanoparticles, Mater. Res. Bull. 41 1310–1318.

[37] Chen. J.Y, Zhou. P.J, Li. J.L, Li. S.-Q, (2007). Depositing Cu_2O of different morphology on chitosan nanoparticles by an electrochemical method, Carbohydr. Polym. 67 623–629.

[38] Ibrahim. M, Alaam. M, Haes. H.E, Jalbout. A.F, Leon. A.d, (2006). Analysis of the structure and vibrational spectra of glucose and fructose, Ecletica Quimica 31 15–21

[39] Keiser. J.T, Brown C.W, Heidersbach R.H, (1982). The electrochemical reduction of rust films on weathering steel surfaces, J. Electrochem. Soc. (1982), http:// dx.doi.org/10.1149/1.2123648.

[40] Li. H, Zhang. Y, Zhang. Q, Wang. Y, Fan. Y, Gao X, Niu. J, (2019). Boosting visible-light Photocatalytic degradation of indomethacin by an efficient and photostable Ag_3PO_4/NG/WO_3 composites, Appl. Surf. Sci. 490: 481–491.

[41] Nandiyanto. A.B.D, Andika. R, Aziz, M., and Riza, L. S. (2019). How to Read and Interpret FTIR Spectroscope of OrganicMaterial. *Indonesian Journal of Science and Technology*, 3(2): 82-94.

[42] Nandiyanto. A. B. D, Andika. R, Aziz, M., and Riza, L. S. (2018). Working Volume and Milling Time on the Product Size/Morphology, Product Yield, and Electricity Consumption inthe Ball-Milling Process of Organic Material. *Indonesian Journal of Science andTechnology*, 3(2): 82-94.

[43] Balamurugan B, Mehta BR, Optical and structural properties of nanocrystalline copper oxide thin films prepared by activated reactive evaporation,*Thin Solid Films;*396:90(2001).